In silico screening of minocycline as an Mpro inhibitor and the adjunctive therapy value for the treatment of COVID-19

Bin Xiao (michael-bin@163.com)
Inner Mongolia Medical Uiversity https://orcid.org/0000-0002-6741-9637
Si Wu
Inner Mongolia Medical University
Yaru Han
Inner Mongolia Medical University
Liwen Ren
Chinese Academy of Medical Sciences & Peking Union Medical College
Jinhua Wang
Chinese Academy of Medical Sciences & Peking Union Medical College Institute of Materia Medica
Xiurong Luan
Inner Mongolia Medical University
Guanhua Du
Chinese Academy of Medical Sciences & Peking Union Medical College Institute of Materia Medica
Zhanfei She
Inner Mongolia Medical University

Research Article

Keywords: COVID-19, old drugs, Mpro, molecular docking, minocycline

Posted Date: April 18th, 2022

DOI: https://doi.org/10.21203/rs.3.rs-1528733/v1

Abstract

To explore potential inhibitors of Severe Acute Respiratory Syndrome-Coronavirus-2 (SARS-CoV-2) for the treatment of novel coronavirus disease (COVID-19), *in silico* screening of 135 clinical drugs was performed targeting on 3-chymotrypsin-like protease (3CLpro, or M^{pro}). Six drugs including anti-HIV drug (raltegravir), antibacterial drugs (cefonicid, cefoperazone, minocycline), and antidiabetic drugs (canaglifozin, glyburide) showed high binding affinities (≤ -8.5 kcal/mol) and interesting binding conformations compared with the designed co-crystal ligand N3 (-7.7 kcal/mol). In which the antibiotic minocycline, an inhibitor of bacterial ribosomal rRNA, showed the highest binding affinity (-9.6 kcal/mol). Valuable hydrogen bonding and hydrophobic interactions were found between minocycline and M^{pro} active site. Beside the hydrogen bond with Cys145, minocycline formed a Pi-Cation with His41, which strongly supported minocycline as a Michael Addition acceptor to bind with the catalytic site of M^{pro}. The structure-affinity relationship was studied based on molecular docking of minocycline analogues. Minocycline showed *in vitro* M^{pro} inhibitory activity with IC_{50} of 5 mM. More importantly, the literature review found that minocycline had both *in vitro* and *in vivo* broad-spectrum antiviral as well as anti-inflammatory activities. Minocycline deserves *in vivo* evaluations as well as randomized controlled trial to investigate the efficacy for the treatment of COVID-19.

Introduction

The novel coronavirus (Severe Acute Respiratory Syndrome-Coronavirus-2, SARS-CoV-2) disease (COVID-19) was first detected in December 2019. As the global ongoing epidemic of SARS-CoV-2, there have been more than 476,000,000 people infected and more than 6,100,000 patients died according to the WHO. COVID-19 is an acute infectious disease with common symptoms including fever, cough, shortness of breath, and dyspnea. In more severe cases, infection causes pneumonia, severe acute respiratory syndrome, kidney failure, or even death [1]. Although the vaccinated population in the world has exceeded 10,900,000,000, to end this catastrophic epidemic, more treatments other than vaccines need to be developed. Remdesivir is the only drug approved by the Food and Drug Administration (FDA) for the treatment of COVID-19. Besides, ritonavir-boosted nirmatrelvir (Paxlovid), molnupiravir, and certain anti-SARS-CoV-2 monoclonal antibodies have been authorized by FDA for emergency use. And the lasted study found that combining pyrimidine biosynthesis inhibitors with antiviral nucleoside analogues synergistically inhibits SARS-CoV-2 infection in vitro and in vivo [2]. As SARS-CoV-2 mutant strains continue to emerge, new therapeutic entities are still needed to be discovered.

The SARS-CoV-2 belongs to the β genus of coronavirus which are enveloped with a positive RNA genome. Potential anti-coronavirus therapies could act on the human immune system/cells or the coronavirus [3]. Non-structure proteins (Nsps) involve in viral RNA transcription, RNA translation, protein synthesis, protein processing and modification, virus replication, and infection of the host [4]. In Nsps, 3-chymotrypsin-like protease (3CLpro, also named as M^{pro}) is automatically cleaved from polyproteins to produce mature enzymes, and further cleaves downstream Nsps at 11 sites to release Nsp 4–16 [5]. The structure and

catalytic mechanism of SARS-CoV M^{pro} allows it as a promising target for anti-coronavirus drug development.

There are three strategies for developing an anti-SARS-CoV-2 drug [6]. The first is to test existing broad-spectrum antivirals for their metabolism, used dosages, efficacy and side effects are clear. However, the side effects of broad-spectrum antivirals should not be underestimated [7]. The second is to high-throughput-screen for SARS-CoV-2 therapeutic candidates from existing clinical 'old drugs' [8, 9]. From this strategy, masitinib was recently discovered as a broad coronavirus 3CL inhibitor that blocked SARS-CoV-2 virus replication [10]. The third is to develop a new drug from scratch, which is theoretically time-consuming [11]. Screening of potential 'old drug' molecules is always a good strategy. Since 'old drug' have been prepared, the medication has sufficient experience, and the safety and pharmacokinetic parameters are well known, with the *in vivo* efficacy in animal model, it could be approved by the Green Channel or the hospital ethics committee for clinical use [3].

In this study, we established a small-scale "old" drug database (clinical drugs being used in Ordos Central Hospital) according to *Linpinski*'s Rule of 5, and conducted *in silico* screening of M^{pro} inhibitors by molecular docking. Binding affinity and interaction as well as structure-affinity relationship were analyzed to better understand the potentiality. *In vitro* M^{pro} inhibition test was conducted based on established method. This study will provide contribution to the transient ongoing infectious disease.

Results And Discussion

Pharmacophore of the co-crystal ligand N3

As illustrated in Figure 1, M^{pro} monomer has three domains: domain Ⅰ (6 antiparallel *β*-sheet), domain Ⅱ (6 antiparallel *β*-sheet) and domain Ⅲ (α-helixes, which are closely related to proteolytic activity), and a long loop connects domains Ⅱ and Ⅲ. A highly conserved substrate-binding pockets (with a Cys145-His41 catalytic dyad) located in a cleft between domains Ⅰ and Ⅱ, suggesting the antiviral inhibitors targeting this site should have broad-spectrum anti-coronavirus activity [12].

As shown in the diagram of Figure 1, a covalent bond between the Sγ atom of Cys145 and the C*β* of the vinyl group is formed, which means the Michael Addition that is critical in the catalytic mechanism has occurred [5]. The lactam functional group at P1 site inserts into the subsite S1 and forms a hydrogen bond with His163, while the functional group Leu at P2 site inserts deeply into the hydrophobic subsite S2 [12]. The functional group Val at P3 site is solvent-exposed tolerating a variety of functional group substitutions. The functional group Ala at P4 side is in a hydrophobic pocket. P5 site makes van der Waals interactions with Pro168, Thr190, and Ala191, while the hydrophobic aromatic ring of N3 forms van der Waals contacts with Thr24 and Thr25. Besides, N3 forms multiple hydrogen bond interactions with the active site residues, helping to lock the inhibitor inside the binding pocket, which determines the inhibition of the enzyme as well as the coronavirus replication [12].

M^{pro}, which is highly conserved among all coronavirus, is a good target for the development of a single antiviral agent or in combination with other potential therapies to provide an effective first line of defense against all coronavirus-associated diseases [13]. The co-crystal structure of SARS-CoV-2 M^{pro} complexed with N3 is a good model for identifying inhibitor lead through *in silico* screening.

In silico screening by AutoDock Vina

For validation of docking simulation, N3 was re-docked into M^{pro}. The described docking workflow allowed top-ranked and reproduced binding conformation which was close to those of the 6LU7 co-crystal structure (checked by PyMOL, RMSD of 1.126 Å). According to AutoDock Vina, binding affinity ≤ -0.0 kcal/mol means the receptor and ligand could automatically bind together. In this study, molecule with binding affinity ≤ -8.5 kcal/mol was treated to be potential based on recent reports on *in silico* screening of SARS-CoV-2 M^{pro} inhibitors [14].

All the 135 'old' drug structures, biological activities, targets, and top-ranked binding affinities were summarized (Supporting information Table. S1). In which, 6 molecules including anti-HIV drug (raltegravir), antibacterial drugs (cefonicid, cefoperazone, minocycline), and antidiabetic drugs (canaglifozin, glyburide) showed high affinities (≤ -8.5 kcal/mol) as well as interesting binding conformations (bound to the M^{pro} active site and formed interesting interactions with key residues). In particular, the antibiotic minocycline, an inhibitor of bacterial ribosomal rRNA, showed the highest binding affinity (-9.6 kcal/mol) compared with N3 (-7.7 kcal/mol). The results indicated that these small molecular drugs might be M^{pro} inhibitors of SARS-CoV-2.

Minocycline is an FDA-approved, second-generation tetracycline class antibiotic with an established safety profile that has been used in clinic for more than 30 years. It acts selectively binding to the 16S rRNA, inhibiting the binding of RNA to ribosomes, and interferes with protein synthesis [15]. The main treatment conditions of minocycline were both gram-positive/negative bacterial infections and the more recent multidrug resistant *Acinetobacter baumannii* [16]. The immune imbalance and bacterial infection often appear in the later stages of COVID-19 progression, the efficacy of antiviral drugs might remain unsatisfactory or insufficient [17]. The antibiotics and glucocorticoid were sometimes administered according to the clinical characteristics and physicians' discretion [18].

Re-docking of N3 and minocycline by Discovery Studio

To gain further validation of the docking simulation, re-docking of known ligand with the target and comparison of docking results generated by different software are academically consensus. From the CDOCKER results generated by Discovery Studio, N3 (Figure 2A) formed conventional hydrogen bonds with residues Phe140, His163, His164, Glu166, Gln189, and Thr190. The isoxazole group formed Pi-Alkyl interaction with Ala191 and Pro168, and hydrophobic aromatic ring formed van der Waals' forces with residues Thr24, Thr25, Leu27 and Cys145. In addition, N3 molecule forms covalent bonds with multiple residues of M^{pro}. The docking results were closely consistent with the co-crystal structure (checked by

PyMOL, RMSD of 1.650 Å), indicating that the CDOCKER docking model was validated and suitable for *in silico* screening of M^{pro} inhibitors.

For minocycline (Figure 2B), it contains multiple hydrophilic groups which formed conventional hydrogen bonding networks with key residues Phe140, Gly143, Cys145, His164, and Glu166 in the active site. The hydrophobic aromatic rings formed van der Waals' forces with multiple amino acid residues of M^{pro}. It is commonly accepted that covalent bond formed between the Cys145-His41 catalytic dyad and the designed compound would increase the M^{pro} inhibition potency, resembling the intermediate during substrate cleavage [5]. Beside the hydrogen bond between Cys145 and 2-carboxamide, a critical Pi-Cation formed between His41 and 4-dimethylamino group, which strongly supported minocycline as a Michael Addition acceptor binding with the exact catalytic site to inhibit M^{pro}. These results indicated that the multiple especially critical interactions stabilized minocycline-M^{pro} in a low energy state, which was required for M^{pro} selection and antiviral activity.

Recent evidence suggested that the precise site of interaction between minocycline and cellular RNA molecules could be double-stranded RNAs (dsRNAs), which have been observed as intermediates of the viral replication of positive-stranded viruses, such as SARS, the aberrant induction of inflammatory cytokines/chemokines in case of SARS infection was mostly activated by dsRNA intermediates [19, 20]. In addition, the robust viral replication and delayed IFN-γ signaling accompanying the initial steps of SARS seem to be consequence of the coronavirus ability to initially evade the host dsRNA-sensors [21, 22]. Therefore, early administration of dsRNA-binding minocycline might reduce the risk of SARS-CoV-2.

Structure-affinity relationship of minocycline

By referring to the literatures from PubMed, Elsevier, Springer, and Google Scholar, a 44-compound (in which 21 compounds were clinical drugs) small-scale database of minocycline analogues was established. After docking simulation, the chemical structures and top-ranked binding affinities of the analogues were summarized (Supporting information Table. S2).

Indeed, minocycline showed a promising highest binding affinity among all the 44 analogues. Structures containing the main octahydrotetracene-2-carboxamide skeleton were analyzed and the structure-affinity relationship was summarized (Figure 3). Carbonyl functional groups should be kept and the middle hydroxyl group might be better if changed to be carbonyl. Furthermore, the terminal 2-carboxamide could be modified with moderate (not too long) moiety. On the 4,7-bis(dimethylamino) side, 4-dimethylamino group is critical for the high affinity, and the *S*-stereochemistry of C4 is better than the *R*-stereochemistry, which was also verified from the previous binding mode investigation that it could form the key covalent bond with His41.

Docking simulation and the structure-affinity relationship study found critical covalent bond formed between the active Cys145-His41 catalytic dyad and minocycline, which helped us to better understand

why the functional groups as well as the tetracycline skeleton could be suitable for the M^{pro} active-site binding and interaction.

In vitro activity assays of the SARS-CoV-2 M^{pro} inhibition

As is shown in Figure 4, minocycline showed a dose-dependent M^{pro} inhibitory activity with IC_{50} of 5mM. Minocycline is an FDA-approved, second-generation tetracycline class antibiotic with an established safety profile, and is used in pharmacological conditions of both bacterial/mycoplasma infections. In spite of this, minocycline appears to have broad-spectrum antiviral activities: reducing West Nile Virus titers in brain-derived cell types, reducing Japanese encephalitis-induced damage in neuronal cells inhibiting H7N9 replication in human lung epithelial cells, and attenuating pathogenic immune responses during infection with human and simian immunodeficiency virus (HIV/SIV) [23, 24-27]. Moreover, based on molecular docking and dynamic studies, minocycline was proposed as potential antiviral therapy against Congo Crimean hemorrhagic fever virus to inhibit the binding of virus to host nucleoprotein [28]. In a randomized controlled trial of dengue hemorrhagic fever patients, compared with standard-of-care, combination therapy with doxycycline (analogue of minocycline) significantly decreased the TNF and IL-6 levels, and mortality [29].

Tetracycline inhibiting pro-inflammatory cytokines and matrix metalloproteinases plays a key role in coronavirus acute infection and is involved in chemokine activation and in tissue destruction [30, 31]. Of note, this immunomodulatory effect seems to be dsRNA-mediated [20]. Besides, minocycline attenuates T cell and microglia activity to impair cytokine production in T cell-microglia interaction [32]. Severe COVID-19 patients were more likely to develop neurological symptoms [33]. ACE2 (the functional receptor for SARS-CoV-2) is present in multiple human organs including nervous system and skeletal muscle [34]. Due to the small size and lipophilic nature, minocycline might cross into tissue compartments with potentially therapeutic concentrations.

The *in vitro* validation result suggesting that the inhibitory activity against SARS-CoV-2 M^{pro} of minocycline might be beneficial in addition to other well-known mechanisms. Further, minocycline could be used as interesting lead to design analogs that can more potently and selectively inhibit SARS-CoV-2 M^{pro} to improve its antiviral activity and avoid the unwanted adverse effects associated with other mechanisms.

Conclusion

In conclusion, from *in silico* screening of 135 clinical drugs targeting on M^{pro} of the novel SARS-CoV-2, minocycline, inhibitor of bacterial ribosomal rRNA, showed interesting binding affinity (-9.6 kcal/mol). Critical hydrogen bonding with the Cys145-His41 catalytic dyad and hydrophobic interactions were found between minocycline and M^{pro} active site. Structure-affinity relationship explained the conformational suitability of minocycline. Minocycline showed *in vitro* M^{pro} inhibitory activity (5 mM). These findings suggested that minocycline, a safe, inexpensive, and readily available antibiotic, deserves *in vivo*

evaluations as well as randomized controlled trial to investigate the efficacy for the treatment of COVID-19. This study shed a new light on an adjuvant treatment strategy for this viral disease.

Experimental

Pharmacophore study of the co-crystal ligand N3

The crystal structure of SARS-CoV-2 M^{pro} in complex with a designed small ligand N3 to 2.1 Å resolution (PDB code: 6LU7) had been determined by Professors Zihe Rao and Haitao Yang's research team from ShanghaiTech University [12]. The protein coordinates of the M^{pro} used in this study were in-time donated by Zihe Rao et al. in Feb, 2020. Based on the structure, key helixes/loops, amino acid residues, and hydrophobic interactions in binding site were investigated and the pharmacophore of N3 was summarized, which was used as a control in the following *in silico* study.

Small-scale drug database

According to *Linpinski*'s Rule of 5, we established a small-scale database including 135 drugs clinically being used in Ordos Central Hospital [35]. Requirement-reached drug 2D structures were drawn by ChemDraw Professional 17.0 software (CambridgeSoft Corporation, Cambridge, MA, USA). The 2D structures of candidates were converted into 3D structural data by Chem3D Ultra 17.0 software (CambridgeSoft Corporation, Cambridge, MA, USA), and all structures of the ligands were energy-minimized.

Molecular docking by AutoDock Vina

We applied a workflow for molecular docking which was described in our previous work [36]. The chain B (co-crystal ligand N3 in 6LU7) and chain C (water molecules) were deleted, and chain A was prepared for docking within the molecular modeling software package Chimera 1.10.2 (National Institutes of Health, Bethesda, MD, USA) [13]. Adding of polar hydrogens and kollman charges, gasteiger computing and grid box parameters defining were done using MGL tools 1.5.6 (The Scripps Research Institute, La Jolla, CA, USA) [37, 38].

All the ligands were set as flexible and the receptor was set as rigid. Docking calculations were performed using AutoDock Vina 1.1.2 software (The Scripps Research Institute, La Jolla, CA, USA) [39]. A search grid box was set to cover the whole surface of M^{pro} protein to collect all possible orientations and conformations of the ligand paired with the protein (including compounds outside the active site). For which, the center was set as: center_x=-23.982, center_y=12.114, center_z=57.466, and the size was set as: size_x=58, size_y=78, size_z=66. Spacing angstrom was set as 1.000, and the exhaustiveness was set as 100. The default settings and the AutoDock Vina scoring function were applied.

Totally 9 binding modes were generated by AutoDock Vina for each compound, and the mode (even outside the active site) with highest binding affinity was selected as the most predictable. Visual

investigation and analysis of ligand-protein interactions were performed using PyMOL V.1.5 (Schrodinger LLC, New York, NY, USA). Binding conformation, affinity, and receptor-ligand interaction were analyzed with N3 as a control.

Re-docking study by Discovery Studio

The accurate 3D protein structure of M^{pro} was defined as the receptor and optimized by hydrogenation, dehydration and removing redundant residues. Location of the originally contained ligand N3 in the co-crystal was defined as the active binding site with a radius as 13.890841 which could cover the best binding region. The X, Y, and Z centers were -10.797, 12.536, and 68.905, respectively. Molecular structure of N3 was also prepared and converted to 3D structure and its energy was minimized. The molecular docking was performed using CDOCKER tool. -CDOCKER_ENERGY and -CDOCKER_INTERACTION_ENERGY was used to score the interaction between receptor and ligand. Discovery Studio 2016 software (Biovia, San Diego, CA, USA) was used for the docking, visualization, and analysis [40].

Structure-affinity relationship of promising drug

Considering the generated information is relatively limited. Investigation of promising drug analogues might provide information for further study such as structure modification. After the *in silico* screening and the re-docking simulation, the analogues of promising drug were collected by referring to literatures from PubMed, Elsevier, Springer, and Google Scholar. Then one-by-one docking of the analogues targeting on M^{pro} was performed. Based on the analogues' binding affinities, the structure-affinity relationship of the promising drug was summarized.

In Vitro Activity Assays of the SARS-CoV-2 M^{pro} Inhibitors

The inhibition rate of compound on M^{pro} enzyme was measured using the 2019-nCoV M^{pro} inhibitors screening kit (P0312S, Beyotime Biotechnology, Shanghai, China) according to the manufacturer's instructions. This kit was monitored at excitation of 340 nm and emission of 490 nm wavelengths on a microplate multimode reader by fluorescence resonance energy transfer. The percentage inhibition of each sample was calculated.

Declarations

The authors declare that they have no conflict of interest.

Acknowledgements

We thank Professors Zihe Rao, Haitao Yang, and Xiuna Yang from ShanghaiTech University for the in time donation of M^{pro} information.

Author contributions

Professors Zhanfei She and Guanhua Du conceptualized and supervised this study. Bin Xiao, Jinhua Wang, and Liwen Ren designed the research, performed virtual screening. Bin Xiao, Si Wu, Liwen Ren, and Jinhua Wang analyzed the docking results analysis. Bin Xiao, Si Wu, and Yaru Han designed and carried out the literature review. Yaru Han performed the *in vitro* M^{pro} inhibitory assay. All authors revised the manuscript, and have read and approved the final manuscript.

Funding

This work was supported by the National Science Foundation for Post-doctoral Scientists of China (2019M650537), the Central Government Funds for Guiding Local Scientific and Technological Development (2020ZY0036), and the Ordos Innovation Fund for Talent Team (Ordos Talent Work Leading Group 2018-No.6, China).

References

1. Xie P, Ma WY, Tang HB, Liu DS (2020) Severe COVID-19: A review of recent progress with a look toward the future. Front Public Health 8:189. doi: https://doi.org/10.3389/fpubh.2020.00189
2. Schultz DC, Johnson RM, Ayyanathan K, Miller J, Whig K, Kamalia B et al (2022) Pyrimidine inhibitors synergize with nucleoside analogues to block SARS-CoV-2. Nat doi. 10.1038/s41586-022-04482-x
3. Wu CR, Liu Y, Yang YY, Zhang P, Zhong W, Wang Y et al (2020) Analysis of therapeutic targets for SARS-CoV-2 and discovery of potential drugs by computational methods, *Acta Pharm Sin B.*, 27;10(5):766–788. doi: 10.1016/j.apsb.2020.02.008
4. Ziebuhr J (2005) The coronavirus replicase. Curr Top Microbiol Innunol 287:57–94. doi: 10.1007/3-540-26765-4_3
5. Yang HT, Xie WQ, Xue XY, Yang KL, Ma J, Liang WX et al (2005) Design of wide-spectrum inhibitors targeting coronavirus main proteases. PLoS Biol 3:e324. doi: 10.1371/journal.pbio.0030324
6. Zumla A, Chan J, Azhar E, Hui D, Yuen K (2016) Coronaviruses-drug discovery and therapeutic options. Nat Rev Drug Discov 15:327–347. doi:10.1038/nrd.2015.37
7. Chan JF, Chan KH, Kao RY, To KK, Zheng BJ, Li CP et al (2013) Broad-spectrum antivirals for the emerging Middle East respiratory syndrome coronavirus. J Infect 67:606–616
8. Wilde AH, Jochmans D, Posthuma CC, Zevenhoven-Dobbe JC, Nieuwkoop S, Bestebroer TM et al (2014) Screening of an FDA-approved compound library identifies four small-molecule inhibitors of Middle East Respiratory syndrome coronavirus replication in cell culture. Antimicrob Agents Chemother 14:4875–4884. doi: 10.1128/AAC.03011-14
9. Dyall J, Coleman CM, Hart BJ, Venkataraman T, Holbrook MR, Kindrachuk J et al (2014) Repurposing of clinically developed drugs for treatment of Middle East respiratory syndrome coronavirus infection. Antimicrob Agents Chemother 58:4885–4893. doi: 10.1128/AAC.03036-14

10. Drayman N, Demarco JK, Jones K, Azizi A, Froggatt S-A, Tan HM (2021) Masitinib is a broad coronavirus 3CL inhibitor that blocks replication of SARS-CoV-2. Science 372(6557):931–936. doi: 10.1126/science.abg5827
11. Omrani AS, Saad MM, Baig K, Bahloul A, Abdul-Matin M, Alaidaroos AY et al (2014) Ribavirin and interferon alfa-2a for severe Middle East respiratory syndrome coronavirus infection: a retrospective cohort study. Lancet Infect Dis 14:1090–1095. doi: 10.1016/S1473-3099(14)70920-X
12. Jin ZM, Du XY, Xu YC, Deng YQ, Liu MQ, Zhao Y et al (2020) Structure of Mpro from COVID-19 virus and discovery of its inhibitors. Nature 582(7811):289–293. doi: 10.1038/s41586-020-2223-y
13. Pettersen EF, Goddard TD, Huang CC, Couch GS, Greenblatt DM, Meng EC et al (2004) UCSF Chimera-a visualization system for exploratory research and analysis. J Comput Chem 25:1605–1612. doi: 10.1002/jcc.20084
14. Zong Y, Ding ML, Jia KK, Ma ST, Ju WZ (2020) Exploring active compounds of Da-Yuan-Yin in treatment of COVID-19 based on network pharmacology and molecular docking method. Chin Tradit Herbal Drugs 51:836–844. doi:10.7501/j.issn.0253-2670.2020.04.002
15. Chukwudi Chinwe U (2016) rRNA binding sites and the molecular mechanism of action of the tetracyclines. Antimicrob Agents Chemother 60:4433–4441
16. Lashinsky JN, Henig O, Pogue JM, Kaye KS (2017) Minocycline for the treatment of multidrug and extensively drug-resistant a. baumannii: A review. Infect Dis Ther 6:199–211. doi: 10.1007/s40121-017-0153-2
17. Huang CL, Wang YM, Li XW, Ren LL, Zhao JP, Hu Y et al (2020) Clinical features of patients infected with 2019 novel coronavirus in Wuhan, China. Lancet 395:15–21. doi: 10.1016/S0140-6736(20)30183-5
18. Ji D, Zhang DW, Chen Z, Xu Z, Zhao P, Zhang MJ et al (2020) Clinical characteristics predicting progression of COVID-19 (2/17/2020). Available at SSRN: https://ssrn.com/abstract=3539674
19. Chukwudi CU, Good L (2016) Interaction of the tetracyclines with double-stranded RNAs of random base sequence: new perspectives on the target and mechanism of action. J Antibiot (Tokyo) 69:622–630. doi: 10.1038/ja.2015.145
20. Ding SW, Voinnet O (2007) Antiviral immunity directed by small RNAs. Cell 130:413–426. doi: 10.1016/j.cell.2007.07.039
21. Cheung CY, Poon LLM, Iris HYN, Luk W, Sia SF, Wu MHS et al (2005) Cytokine responses in severe acute respiratory syndrome coronavirus-infected macrophages in vitro: possible relevance to pathogenesis. J Virol 79:7819–7826. doi: 10.1128/jvi.79.12.7819-7826.2005
22. Deng XF, Hackbart M, Mettelman RC, O'Brien A, Mielech AM, Yi GH et al (2017) Coronavirus nonstructural protein 15 mediates evasion of dsRNA sensors and limits apoptosis in macrophages. PNAS 114:E4251–E4260. doi: 10.1073/pnas.1618310114
23. Drewes JL, Szeto GL, Engle EL, Liao ZH, Shearer GM, Zink MC et al (2014) Attenuation of pathogenic immune responses during infection with human and simian immunodeficiency virus (HIV/SIV) by the tetracycline derivative minocycline. PLoS ONE 9:e94375. doi: 10.1371/journal.pone.0094375

24. Michaelis M, Kleinschmidt MC, Doerr HW, Jr JC (2007) Minocycline inhibits West Nile virus replication and apoptosis in human neuronal cells. J Antimicrob Chemother 60:981–986. doi: 10.1093/jac/dkm307
25. Mishra MK, Ghosh D, Duseja R, Basu A (2009) Antioxidant potential of minocycline in japanese encephalitis virus infection in murine neuroblastoma cells: correlation with membrane fluidity and cell death. Neurochem Int 54:464–470. doi: 10.1016/j.neuint.2009.01.022
26. Josset L, Zeng H, Kelly SM, Tumpey TM, Katze MG (2014) Transcriptomic characterization of the novel avian-origin influenza A (H7N9) virus: specific host response and responses intermediate between avian (H5N1 and H7N7) and human (H3N2) viruses and implications for treatment options. mBio 5:e01102–e01113. doi: 10.1128/mBio.01102-13
27. Hendricks K, Parrado MG, Bradley J (2020) Opinion: An existing drug to assess in vivo for potential adjunctive therapy of Ebola Virus disease and post-Ebola syndrome. Front Pharmacol 10:1691. doi: 10.3389/fphar.2019.01691
28. Sharifi A, Amanlou A, Moosavi-Movahedi F, Golestanian S, Amanlou M (2017) Tetracyclines as a potential antiviral therapy against Crimean Congo hemorrhagic fever virus: Docking and molecular dynamic studies. Comput Biol Chem 70:1–6. doi: 10.1016/j.compbiolchem.2017.06.003
29. Fredeking TM, Zavala-Castro JE, González-Martínez P, Moguel-Rodríguez W, Sanchez EC, Foster MJ et al (2015) Dengue patients treated with doxycycline showed lower mortality associated to a reduction in IL-6 and TNF levels. Recent patents on anti-infective drug discovery. Recent Pat Antiinfect Drug Discov 10:51–58. doi: 10.2174/1574891x10666150410153839
30. Griffin MO, Fricovsky E, Ceballos G, Villarreal F (2010) Tetracyclines: a pleitropic family of compounds with promising therapeutic properties. Am J Physiol Cell Physiol 299:C539–C548. doi: 10.1152/ajpcell.00047.2010
31. Marten NW, Zhou JH (2005) The role of metalloproteinases in corona virus infection. Experimental Models of Multiple Sclerosis 839–848. doi: 10.1007/0-387-25518-4_48
32. Giuliani F, Hader W, Yong VW (2005) Minocycline attenuates T cell and microglia activity to impair cytokine production in T cell-microglia interaction. J Leukoc Biol 78:135–143. doi: 10.1189/jlb.0804477
33. Mao L, Jin HJ, Wang MD, Hu Y, Chen SC, He QW et al (2020) Neurological Manifestations of Hospitalized Patients with COVID-19 in Wuhan, China: a retrospective case series study. JAMA Neurol 77:1–9. doi: 10.1001/jamaneurol.2020.1127
34. Zhao Y, Zhao ZX, Wang YJ, Zhou YQ, Ma Y, Zuo W (2020) Single-cell RNA expression profiling of ACE2, the receptor of SARS-CoV-2. Am J Respiratory Crit Care Med 202(5):756–759. doi: 10.1164/rccm.202001-0179LE
35. Lipinski CA, Lombardo F, Dominy BW, Feeney PJ (1997) Experimental and computational approaches to estimate solubility and permeability in drug discovery and development settings. Adv Drug Deliv Rev 23:3–25. doi: 10.1016/s0169-409x(00)00129-0

36. Xiao B, Wang SM, She ZF, Cao QF, Zhao N, Tian XR et al (2017) Structure-based design, synthesis, PPAR-γ activation, and molecular docking of *N*-substituted phthalimides. Med Chem Res 26:1628–1634. doi:10.1007/s00044-017-1867-0
37. Sanner MF (1999) Python: a programming language for software integration and development. J Mol Graphics Mod 17:57–61 PMID: 10660911
38. Morris GM, Huey R, Lindstrom W, Sanner MF, Belew RK, Goodsell DS et al (2009) AutoDock4 and AutoDockTools4: Automated docking with selective receptor flexibility. J Comput Chem 30:2785–2791. doi: 10.1002/jcc.21256
39. Trott O, Olson AJ (2010) AutoDock Vina: improving the speed and accuracy of docking with a new scoring function, efficient optimization, and multithreading. J Comput Chem 31:455–461. doi: 10.1002/jcc.21334
40. Chowdhury KH, Chowdhury MR, Mahmud S, Tareq AM, Hanif NB, Banu N, Reza ASMA, Emran TB, Simal-Gandara J (2020) Drug repurposing approach against novel coronavirus disease (COVID-19) through virtual screening targeting SARS-CoV-2 main protease. Biology 10:2. doi:10.3390/biology10010002

Figures

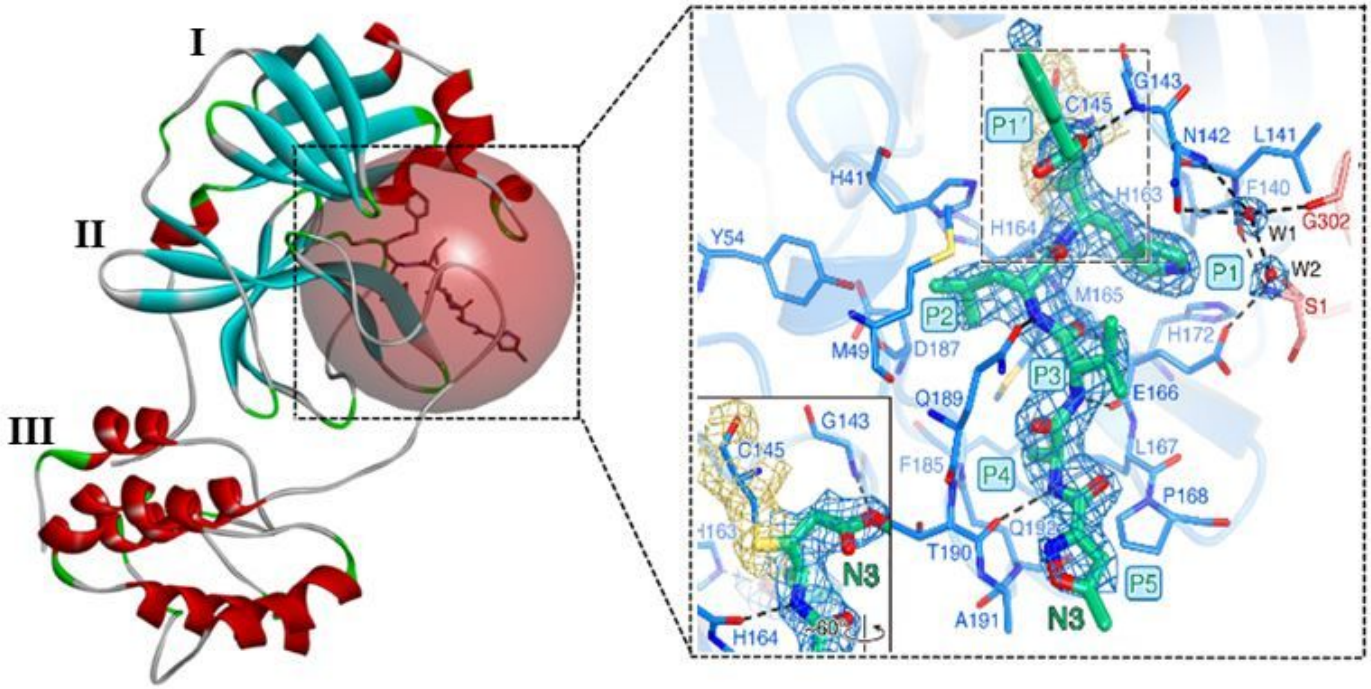

Figure 1

N3 bound in M^{pro} active site and the diagram of the interactions in the co-crystal [12]**.** P1, P1', P2, P3, P4 and P5 sites of N3 are indicated, 2Fo-Fc density map is shown around N3 molecule in blue mesh, C145-A

in yellow mesh, and water in blue mesh. The key residue is shown in stick, hydrogen bond is shown in black dashed line, and water is shown as red sphere.

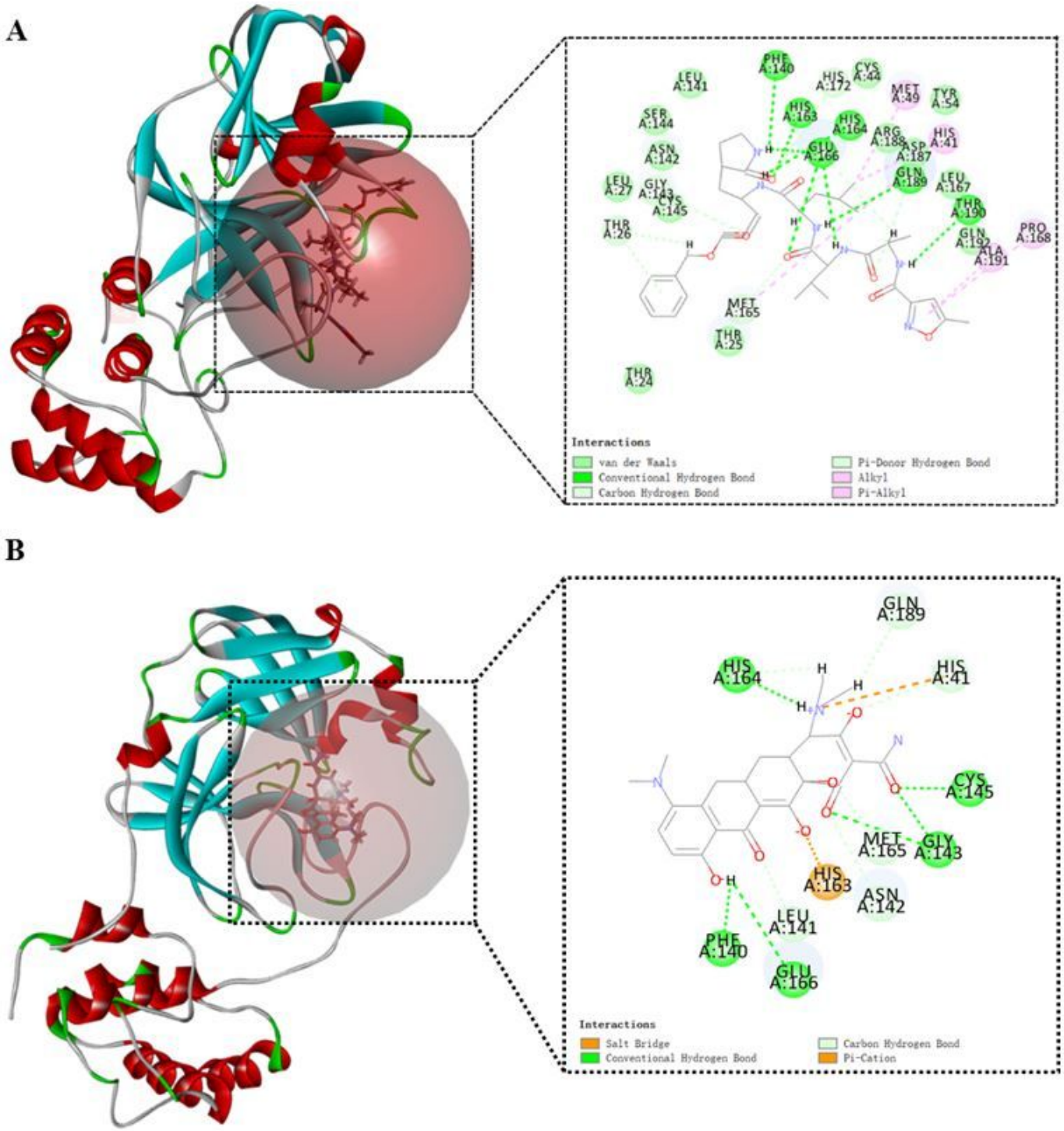

Figure 2

(A) Diagram of the interactions between N3 and M^{pro}; (B) Diagram of the interactions between minocycline and M^{pro}. The key amino acid residue is shown in sphere; Salt-bridge is shown in orange

dashed line; Conventional hydrogen bond is shown in green dashed line; Carbon hydrogen bond is shown in light blue dashed line; Pi-cation is shown in bright-orange dashed line.

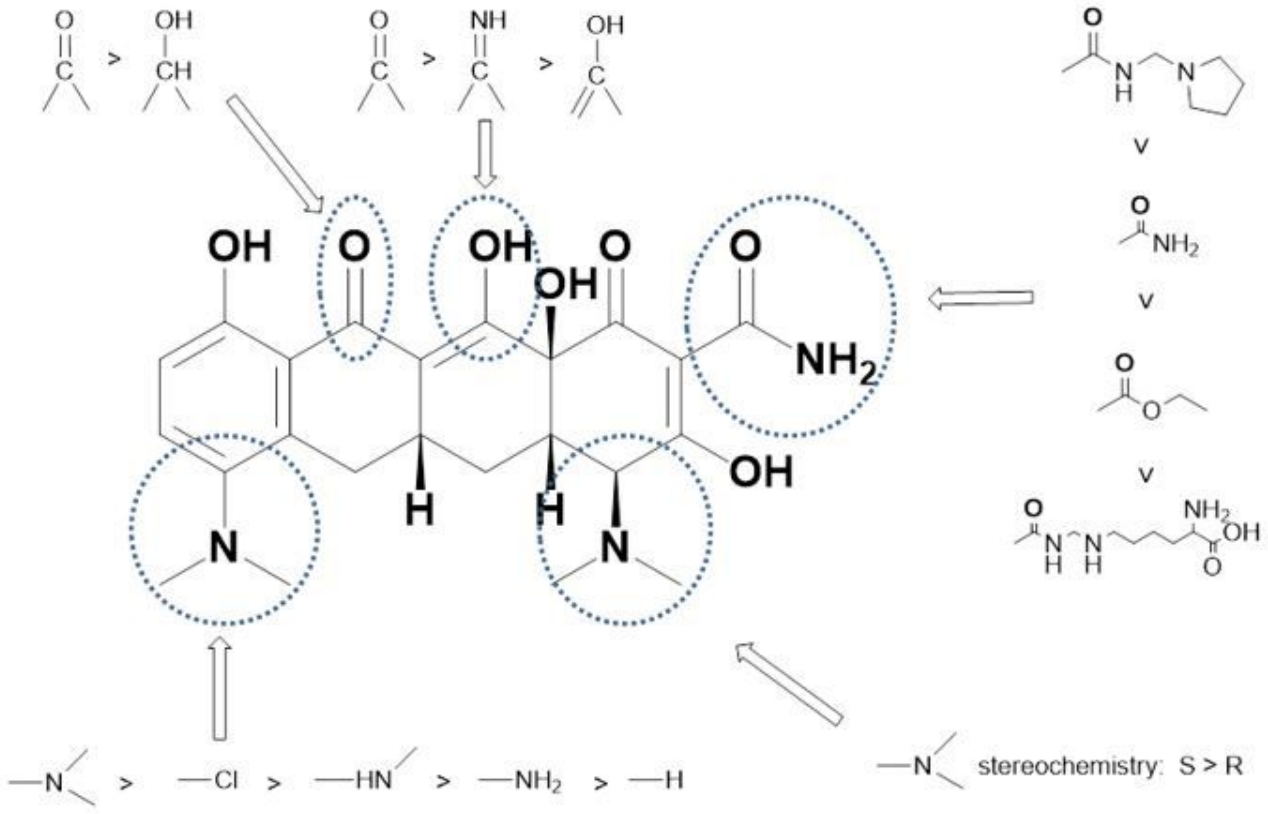

Figure 3

Primary structure-affinity relationship illustration of minocycline targeting on M^{pro}.

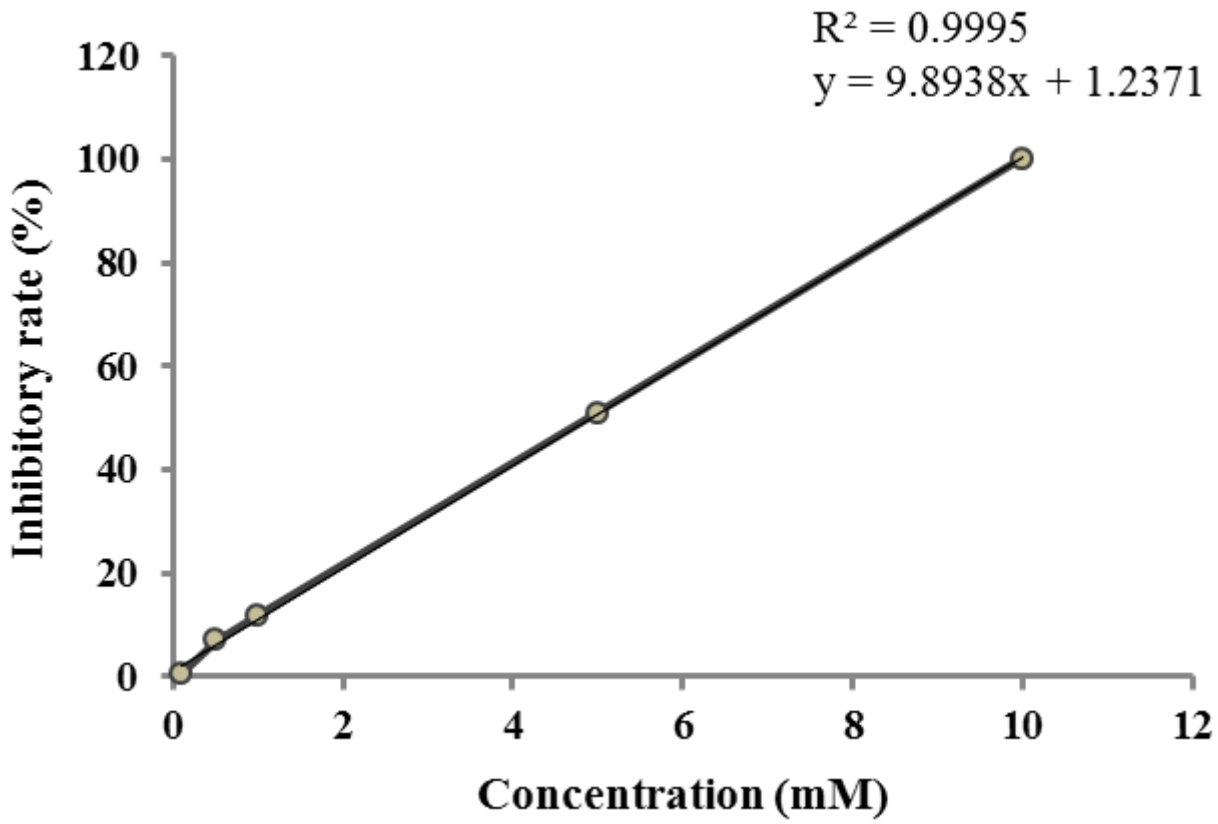

Figure 4

In vitro validation of the inhibitory activity of minocycline on M^{pro}.

Supplementary Files

This is a list of supplementary files associated with this preprint. Click to download.

- Graphicalabstract.docx
- SupportinginformationTableS1.doc
- SupportinginformationTableS2.docx